Biogeochemistry (2017) 135:307–324
DOI 10.1007/s10533-017-0376-z

Contributions of freshwater mussels (Unionidae) to nutrient cycling in an urban river: filtration, recycling, storage, and removal

Timothy J. Hoellein · Chester B. Zarnoch · Denise A. Bruesewitz · Jessi DeMartini

Received: 22 June 2017 / Accepted: 2 September 2017 / Published online: 9 September 2017

Abstract Consumers contribute to nutrient cycling in aquatic ecosystems by nutrient retention in tissues, metabolic transformations and excretion, and promoting microbial processes that remove nutrients (i.e., nitrogen (N) loss via denitrification). Freshwater mussels (Unionidae) form dense assemblages in rivers, and affect nutrient transformations through feeding, biodeposition, and bioturbation. However, the effects of Unionid mussels on N and phosphorus (P) retention are not commonly measured. We quantified rates of filtration, retention, and biodeposition of carbon (C), N, and P for two Unionid species: *Lasmigona complanata* and *Pyganodon grandis*. We used continuous-flow cores with ^{15}N tracers to measure denitrification in sediments alone and with a single individual of each species. We conducted measurements in an urban river near Chicago, IL, USA that is a target for Unionid restoration. Both Unionid species showed high rates of P-specific feeding and retention, but low N-specific rates. This was in agreement with high N:P ratio in the water column. Each species significantly increased denitrification relative to sediment alone. ^{15}N tracers suggested direct denitrification of nitrate increased denitrification, although enhanced coupled nitrification–denitrification likely also contributed to denitrification. Finally, denitrification rates with and without mussels were used to estimate the value of N loss under different scenarios for mussel restoration at the river scale. Overall, restored Unionid populations may enhance P retention in soft tissues and shells and N loss via denitrification. Ecosystem managers may find greater support for restoration of Unionid populations with careful calculations of their ecosystem role in nutrient retention and removal.

Keywords Bivalves · Biodeposits · Clearance rate · Eutrophication · Consumers · Stoichiometry

Responsible Editor: Breck Bowden.

T. J. Hoellein (✉)
Department of Biology, Loyola University Chicago, 1032 W Sheridan Rd, Chicago, IL 60660, USA
e-mail: thoellein@luc.edu

C. B. Zarnoch
Department of Natural Sciences, Baruch College and Graduate Center, City University of New York, 17 Lexington Ave, Box A-0506, New York, NY 10010, USA
e-mail: chester.zarnoch@baruch.cuny.edu

D. A. Bruesewitz
Environmental Studies Program, Colby College, 4000 Mayflower Hill, Waterville, ME 04901, USA

J. DeMartini
Office of Natural Resources, Urban Stream Research Center, Forest Preserve District of DuPage County, Warrenville, IL 60555, USA
e-mail: jessidemartini@dupageforest.org

Introduction

Animals produce 'hot spots' and 'hot moments' of biogeochemical cycling by altering nutrient availability via feeding, excretion, migration, and death (Janetski et al. 2009; McIntyre et al. 2008; Small et al. 2011). In addition, animals can affect microbially-mediated nutrient transformations through their effects on hydrology, primary production, decomposition, stoichiometry, and redox conditions (Atkinson et al. 2014; Hall et al. 2003; Levi et al. 2013). The influence of animals on biogeochemistry can sometimes be quantified following changes to community composition or species abundance. Invasive species (Capps and Flecker 2013; Strayer et al. 1999), extirpation of native taxa (Strayer 2014), and restoration of historically abundant organisms (Kellogg et al. 2013) have revealed consumers' role in nutrient cycling.

Denitrification, or the reduction of nitrate (NO_3^-) to di-nitrogen gas (N_2), is a major focus of research in aquatic ecosystems because it is a permanent removal of bioreactive nitrogen (N). Denitrification requires organic carbon (C), NO_3^-, and anoxia (Groffman et al. 1999), all of which may be affected by animal consumers. For example, the role of freshwater bivalves on nutrient cycling has received research attention, given the high biomass and variable population size of both invasive and native taxa (Strayer 2014; Strayer et al. 1999; Vaughn and Hakenkamp 2001). Bivalves may stimulate denitrification via waste production, enhanced exchange of water column solutes with sediment microbes, and activity of gut- and shell biofilms. Feces and pseudofeces (i.e., biodeposits) are rich in organic C, organic N, and ammonium (NH_4^+), and biodeposit C may serve as a substrate for denitrification of water column NO_3^- (Hoellein and Zarnoch 2014) and can enhance sediment respiration, creating redox conditions needed for denitrification. In addition, NH_4^+ can be directly excreted or mineralized from biodeposits, nitrified and then denitrified (coupled-nitrification–denitrification). Infaunal bivalves can also enhance denitrification if their burrowing and pedal feeding enhances delivery of water column NO_3^- into the sediment for denitrifying microbes or alter sediment oxygen profiles (Turek and Hoellein 2015; Welsh et al. 2014). Finally, microbes in bivalve guts and shell biofilms conduct nitrification and denitrification (Heisterkamp et al. 2013; Svenningsen et al. 2012).

Freshwater mussels (Unionidae) are long-lived, and their dense, multi-species communities historically constituted the majority of macroinvertebrate biomass in many North American rivers (Vaughn et al. 2008). Other bivalve taxa which form dense populations in freshwaters (e.g., invasive mussels and clams) can promote N storage, burial, and denitrification. For example, zebra mussels (*Dreissena polymorpha*) enhance coupled nitrification–denitrification (Bruesewitz et al. 2008) and reduce NO_3^- limitation of denitrification (Bruesewitz et al. 2009). The invasive Asian clam (*Corbicula fluminea*) increases nitrification (Zhang et al. 2011), denitrification, and NH_4^+ flux (Turek and Hoellein 2015). Storage of N and phosphorus (P) in Unionid soft tissues and shells can be major sites of nutrient retention at the river scale (Atkinson and Vaughn 2015). Unionid consumers are hypothesized to affect denitrification, but their influence on denitrification rates and pathways is unknown. Understanding the nutrient dynamics of Unionid ecology is critical as they are among the most highly imperiled taxa in freshwaters (Lydeard et al. 2004). A detailed assessment of Unionids' potential to improve water quality may provide economic incentives for funding conservation or restoration of these populations.

Our understanding of the Unionids' role in N cycling can benefit from new techniques and perspectives from marine bivalve ecology. For example, oysters have been extirpated in coastal ecosystems worldwide (Beck et al. 2011), and restoration of native oyster reefs is commonplace to recover lost ecosystem services, including their potential to promote denitrification (Grabowski and Peterson 2007; Kellogg et al. 2014). Thus, interest in oyster conservation and restoration has supported a major expansion in research on their role in ecosystem processes (reviewed by Kellogg et al. 2014). Results demonstrated that the influence of oysters on sediment denitrification is context-dependent, and varies according to habitat (Smyth et al. 2015), water chemistry (Hoellein and Zarnoch 2014), and feeding rates (Hoellein et al. 2015). Like oysters, Unionid mussels have experienced widespread extirpation and extinction, and there is interest in their conservation and restoration. Because the role of Unionids in denitrification pathways is rarely explored (Benelli et al. 2017), we

applied the same well-developed analytical tools from oyster research to measure feeding, biogeochemistry, (i.e., ^{15}N tracers and continuous-flow chambers), and ecosystem services (Beseres Pollack et al. 2013) for Unionid mussels.

Our objectives were to characterize the role Unionid species play in nutrient retention and removal in a high-nutrient urban river that is a target for future Unionid restoration. We measured rates of filtration, retention, and biodeposition of C, N, and P for two common Unionid species: *Lasmigona complanata* (white heelsplitter) and *Pyganodon grandis* (giant floater). We also used continuous-flow cores with ^{15}N tracers to measure denitrification pathways in sediments alone and in sediment with a single individual of each species. We predicted mussels would be a net sink of nutrients, where tissues and shell biomass represented a major standing stock of C, N, and P at the reach scale (Atkinson and Vaughn 2015). We also expected that mussels would enhance N_2 production via direct denitrification, where denitrification of water column NO_3^- would be enhanced by either (1) increased sediment organic matter quality and quantity from biodeposits, and/or (2) increased exchange of water column nutrients to sediment denitrifiers via burrowing and bioturbation (Hoellein et al. 2015; Turek and Hoellein 2015).

Methods

Study site and mussel density

The study was conducted in the East Branch of the DuPage River at the Hidden Lake Forest Preserve of DuPage County, just downstream of its confluence with Lacey Creek (Downers Grove, IL, USA; latitude 41.8280848, longitude −88.0497874). The river at this site is a third–fourth order stream. The site was chosen because the mussel population was well documented by previous Forest Preserve research (Jessi DeMartini, personal communication). The East Branch DuPage River is in the Chicago Metropolitan Region, and land-use in the watershed is primarily residential (41.4% of watershed land-use), and includes infrastructure (20.6%), and industry, commercial, and institutional land-use (16.4%). Conservation and open space is 21.6% of the watershed, and agriculture land-use is 0.44% (DuPage County Stormwater Management 2015).

We measured physicochemical characteristics and mussel community composition on June 9, 2014. We marked transects every 10 m along the 60 m reach, and measured water depth every 2 m across each transect. We quantified the stream discharge at 1 location in the reach by measuring the depth and water velocity at 2 m intervals across a transect. For water column nutrients, we filtered three stream water samples with a 60 mL syringe and 0.2 µm nylon filters (Thermo Scientific, Rockwood, TN, USA) into acid-washed 20 mL plastic scintillation vials. Nylon filters were rinsed with several millilitres of sample water prior to filtering into scintillation vials. Samples were kept on ice and frozen upon returning to the laboratory.

We set up 5 × 5 m quadrats at four random locations in the study reach to quantify mussel community composition and density. Corners of each quadrat were marked with rebar and mussels were collected by slowly crawling through the quadrat using gloved hands to search the top 10 cm of sediment. Mussels were gently removed and placed in a bucket. Each quadrat was searched three times by two different researchers to ensure complete collection. We recorded the species and shell height of each individual. Some were reserved for feeding measurements and continuous-flow cores (see below), all others were returned to their quadrat of origin.

We collected sediment samples (N = 5) to a depth of 2.5 cm from each plot using a 2.5 cm diameter corer. Sediment was frozen at −20 °C until analysis of ash-free dry mass (AFDM), elemental composition, and chlorophyll *a*. Subsamples were dried at 60 °C and then used for elemental analysis (C, N, P) or were ashed at 500 °C and reweighed to determine AFDM. Analyses of C and N were performed on a Series II 2400 CHN Analyzer (Perkin Elmer Life and Analytical Sciences, Shelton, CT) using acetanilide as a standard. Sediment P content was determined by sample combustion (500 °C), acid hydrolysis (Aspila et al. 1976), and then measurement of soluble reactive P colorimetrically (Murphy and Riley 1962) using a Seal AQ2+ discrete analyzer (Seal Analytical, Inc., Mequon, WI). Sediment subsamples from the plots were also used to measure chlorophyll *a*. Samples were treated with 90% acetone, sonicated, extracted overnight at 4 °C, and measured spectrophotometrically

(Parsons et al. 1984). Sediment from the analysis was dried at 60 °C and weighed to normalize chlorophyll *a* to sediment mass.

Element standing stocks

We calculated standing stock of C, N, and P at the reach scale for sediment, mussel tissue, and mussel shells. We first converted sediment AFDM and mass of C, N, and P from volume-based (g mL^{-1}) to area-based units (g m^{-2}). The continuous-flow cores had 150 mL of sediment (depth = 5 cm) with a surface area of 0.0045 m^2 (see below). We used this volume to area ratio to convert the relative abundance of each element in the cores into the mass of each element in the top 5 cm of sediment of the stream reach area. The 5 cm depth represents the zone of mussel burial and is a primary zone of denitrification for streams in this region (Inwood et al. 2005). We acknowledge this is 2.5 cm deeper than our sediment collection depth, but assert minimal differences in sediment composition between 0–2.5 and 2.5–5 cm depth. We scaled the elemental content within mussels to the stream reach scale using length measurements from all individual mussels (i.e., length-mass regressions), summed for each 5 × 5 m plot, and averaged per m^2 for each taxon in the reach.

Mussel feeding and biodeposition

Mussel feeding measurements were performed with the "biodeposition method" (Bayne 2002; Bayne et al. 1999; Iglesias et al. 1998), where seston inorganic matter is considered a conservative tracer and characterization of seston and mussel biodeposits (i.e., feces and pseudofeces) allows for quantifying feeding behavior. A complete description of the feeding method is described in Hoellein et al. (2015). Briefly, tables with feeding trays (n = 16) were setup on a path adjacent to the river. The trays were shaded by the forest canopy during the feeding trials. A submersible pump (Danner Supreme(R), Model MD18, Islandia, NY, USA) was deployed into the river to pump water through each feeding tray (450 ± 50 mL min^{-1}). A single mussel was placed in each tray and allowed to feed as indicated by valve gape and biodeposit production. After each mussel consistently produced biodeposits we cleaned the trays by siphoning, and began timed trials (30–45 min) by collecting all feces and pseudofeces separately by pipette without disturbing the mussels. Continuous collection of biodeposits and tray design minimized the chance for biodeposits to flow out of the trays before collection (Bayne 2002; Hoellein et al. 2015). We completed feeding measurements for 21 mussels (N = 10 *L. complanata* and N = 11 *P. grandis*).

Feces and pseudofeces from each mussel were filtered separately on previously ashed and weighed glass fiber filters (GF/F) which were placed in a 47 mm Petri dish and frozen at −20 °C until analysis. We performed two sequential feeding trials for each mussel. Filters with biodeposits from the first trial were dried at 60 °C, weighed, combusted at 450 °C, and weighed again to determine inorganic and organic content of the feces and pseudofeces. Biodeposits from the second trial were dried at 60 °C and used to measure C, N, P content as described above. Seston samples (200 mL) were filtered onto previously ashed and weighed GF/F for elemental analysis (n = 3) and for measurement of organic and inorganic content. Analyses performed on each seston filter were similar to those described for the biodeposits. A filter blank for the CHN analyzer was created by passing 200 mL of filtered (0.45 μm) river water through a GF/F.

Measurement of biodeposit mass and elemental content allowed us to determine total biodeposition rates (mg h^{-1}) as well as biodeposit (feces and pseudofeces) specific rates. We combined these measurements and the seston analyses to derive feeding rates and efficiencies (Bayne 2002; Bayne et al. 1999; Hoellein et al. 2015). Feeding rates were standardized to the mean dry mass of each species using their tissue dry weight and the allometric exponent of b = 0.88 (Kryger and Riisgård 1988). Thus, each feeding rate represents a standard individual mussel (Baker and Levinton 2003) for each species in the study reach.

Mussel excretion and nutrient content

A subset of the mussels collected for the feeding trials were used in excretion measurements (N = 3 *L. complanta* and N = 4 *P. grandis*). Shells were scrubbed under running DI water and each mussel was placed individually in beakers containing filtered (0.45 μm) river water. Each beaker was gently aerated. We began a timed excretion trial (1.75 h) when a mussel's valves were gaping. Excretion rates were calculated as the difference in NH_4^+ between containers with mussels and control containers (N = 3) without mussels. We note that the small

sample size for these measurements, attributed to (1) minimizing impact on the river's sensitive mussel populations, and (2) the excretion experiments were performed concurrently with core incubations (see below) which required the majority of collected individuals.

We recorded shell length (longest axis), width, and depth from all mussels used in feeding and excretion measurements. The wet weight of each individual (shell + tissue) was measured and the tissue and shell were separated and weighed individually. Tissue and shell were dried at 60 °C, weighed, and ground into a powder. Elemental analyses (C, N, P) were performed for the tissue and shell of each individual as described above. Elemental content (i.e., total, tissue, shell) for each species was then calculated at the scale of the individual (i.e., g individual^{-1}), and for the stream reach (i.e., g m^{-2}) using the density of each species.

Sediment cores and continuous-flow analyses

To set up continuous-flow cores, we followed the protocol in Turek and Hoellein (2015; Fig. 1 in that paper), modified from Gardner and McCarthy (2009). We collected homogenized sand and small gravel from the top 5 cm of sediment at the study site. Any macroinvertebrates, including mussels or clams (*Corbicula fluminea*) were removed. We also collected 6, 20-L carboys of unfiltered site water. Sediment and site water were returned to the laboratory within 3 h.

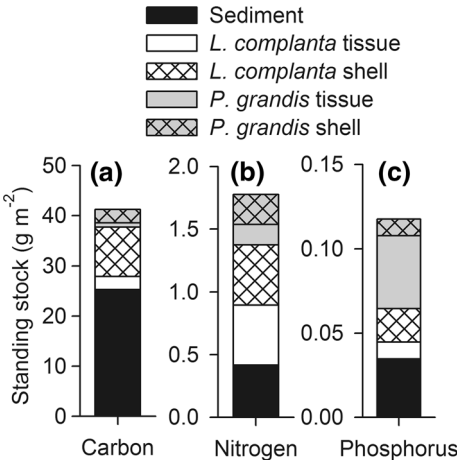

Fig. 1 Standing stock of (**a**) carbon, (**b**) nitrogen, and (**c**) phosphorus at the stream reach scale for sediment, tissue, and shell content of *L. complanata* and *P. grandis*

In the laboratory, we placed 150 mL of homogenized sediment in an acrylic core (30 × 7.6 cm; N = 18 cores). We gently filled each core with 250 mL of unfiltered site water (~5 cm above the sediment–water interface). We added a single live *L. complanta* or a single *P. grandis* to 12 of the cores, while the other six cores had sediment only. A plunger was placed inside each core which contained a rubber O-ring on the sides and polyetheretherketone inlet and outlet tubing (Zeus Inc., Branchburg, NJ, USA). We established three treatments in the inflow water (N = 3 cores per treatment): control (no isotope), $+^{15}NH_4^+$ (+20 μM $^{15}NH_4^+$-N; 98 atom % ^{15}N), and $+^{15}NO_3^-$ (+20 μM $^{15}NO_3^-$N; 98 atom % ^{15}N). As a result, we had a fully crossed experiment with two factors: inflow water (control, $^{15}NH_4^+$, or $^{15}NO_3^-$) and mussels (sediment alone, *L. complanta*, or *P. grandis*). We pumped aerated site water through the cores for 24 h (1.1 mL min^{-1}) at room temperature (21 °C). All cores were incubated in the dark to avoid formation of bubbles via photosynthesis.

After 24 h, we collected water for measurements of dissolved nutrients and gases. For nutrients, we filtered water from each inflow and outflow into 20 mL scintillation vials (0.2 μm nylon filters, Thermo Scientific, Rockwood, TN, USA; N = 3) and froze vials until measurement of NH_4^+, nitrite (NO_2^-), NO_3^-, and soluble reactive phosphorus (SRP). For dissolved gases, we collected inflow and outflow water into 3, 12 mL exetainers (Labco Ltd., Lampeter, United Kingdom). Tubes were filled slowly from the bottom and allowed to overflow for several volumes. We added 200 μL of 50% zinc chloride (McCarthy et al. 2007) and capped the exetainers while making sure there were no bubbles in the headspace. Vials were stored underwater and below room temperature. Mussel feeding was observed in all individuals during continuous-flow measurements, and no mussels died. Due to equipment limitation, we ran 12 cores immediately after collection in the field, and the last six cores immediately after the first 12 were completed. To minimize any effect of the 24 h delay on the final six cores, we had one core of each water and sediment combination on day 2. We sampled after 24 h based on previous studies using identical equipment (Bruesewitz et al. 2013; Hoellein et al. 2015; McCarthy and Gardner 2003), but we note that steady state conditions were not directly measured after 24 h. After water collection, we dismantled the cores and collected the

top 2–3 cm of sediment from each. Sediment and mussels were frozen for elemental analyses and AFDM as described above.

Dissolved inorganic nutrients were measured on an Autoanalyzer III (Seal Analytical, Inc., Mequon, WI) using the phenol hypochlorite technique for NH_4^+ (Solorzano 1969), the antimonyl tartrate method for SRP (Murphy and Riley 1962), and the sulfanilimide method for NO_2^- (without cadmium reduction) and $NO_2^- + NO_3^-$ (with cadmium reduction) (APHA 1998). Dissolved gases were measured using membrane inlet mass spectrometry (MIMS; Bay Instruments, Easton, MD, USA; Kana et al. 1998). The mass spectrometer measured $^{28}N_2$, $^{29}N_2$, $^{30}N_2$, $^{32}O_2$, and ^{40}Ar abundance. Standards were water, maintained at constant temperature, equilibrated to the atmosphere for 24 h prior to measurement (Lab Egg RW11 Basic, IKA Works, Inc., Wilmington, NC, USA). We corrected for instrument drift with standard checks every 10 samples. When N_2 is present, the MIMS's quadrupole mass spectrometer can produce O+ which forms nitric oxide (NO) that can affect $^{28}N_2$ and $^{30}N_2$ results (Eyre et al. 2002; Kana and Weiss 2004). However, no mass 30 production (which would indicate nitric oxide) was detected in cores without $+^{15}N$, so we assume the effect is negligible (McCarthy et al. 2008). Finally, we note N_2 produced via anammox is not distinguishable from denitrification using this method, and that N_2 flux does not account for incomplete denitrification to nitrous oxide. In flowing waters, annamox and nitrous oxide production are minor gas fluxes relative to denitrification (Beaulieu et al. 2011).

Fluxes of nutrients and gases were calculated as the difference in concentration from the outflow and inflow, accounting for pump flow rate and core surface area, to generate flux in units of μg element m^{-2} h^{-1}. A positive value indicates net production or flux out of the sediment and net retention is a negative value. For all rates, we calculated flux for each core using three analytical replicates, and the three replicate cores were the experimental units for each treatment (Bruesewitz et al. 2013; Gardner and McCarthy 2009). Flux detection limits were set at the rate at which SE did not overlap with zero (after Gardner and McCarthy 2009). We used control cores (no added ^{15}N) to report denitrification and respiration rates. We used calculations reported in An et al. (2001) for simultaneous N-fixation and denitrification in $+^{15}NO_3^-$ cores, although we measured no N-fixation in any cores. Potential denitrification was the total $^{28}N_2$, $^{29}N_2$, $^{30}N_2$ production with added $^{15}NO_3^-$. The $^{29}N_2 + {}^{30}N_2$ produced with added $^{15}NO_3^-$ was an index of direct denitrification of NO_3^-, the $^{29}N_2 + {}^{30}N_2$ produced with added $^{15}NH_4^+$ was an index of coupled nitrification–denitrification (Hoellein et al. 2015).

We calculated potential dissimilatory NO_3^- reduction to $^{15}NH_4^+$ (DNRA) from measured ^{15}N:^{14}N ratios in the NH_4^+ from cores that were amended with $^{15}NO_3^-$. Ratios of ^{15}N:^{14}N were measured using time-of-flight mass spectrometry and NH_4^+ complexed with indophenol to increase the mass of the N. We used calculations as detailed in Bruesewitz et al. (2015) which incorporate the isotopic ratios and concentrations of each solute in inflow and outflow water. The DNRA rate is a potential value because of the elevated NO_3^- concentrations from the ^{15}N amendment, but are also considered conservative because we did not measure pore-water NH_4^+ or loss of $^{15}NH_4^+$ from cation exchange (Bruesewitz et al. 2013; Gardner et al. 2009).

Statistical analyses

We used a 2-way ANOVA to quantify the influence of inflow water (control, $^{15}NH_4^+$, $^{15}NO_3^-$) and mussel treatment (sediment alone, *L. complanata*, and *P. grandis*) on sediment characteristics and fluxes of inorganic nutrients and gases. We used Tukey's multiple comparison test following a significant effect of water or mussel treatment. If there was a significant water x mussel interaction, we used a 1-way ANOVA for each mussel treatment individually, with a Bonferonni-correction to adjust the p value for multiple comparisons (i.e., $0.05/3 = 0.017$) (Zar 1999).

Results

The study site had high nutrients and conductivity typical of urban streams (Table 1). Seston particulate matter and sediment organic content was 58.7 mg L^{-1} and 5.2%, respectively, and water column chlorophyll *a* was 27 μg L^{-1}, suggesting food availability for mussels was high. Daytime DO concentration was elevated (119% saturation), likely reflecting primary production in the study reach and in the upstream wetlands and impoundments (Table 1).

Mussel density, standing stock, feeding, and biodeposition

Mussel surveys showed the reach was dominated by two species, where *L. complanata* density was three times greater than *P. grandis* (Table 2). The only other species found was two individuals of *Utterbackia imbecillis* (paper pondshell). On an individual basis, *P. grandis* biomass was higher than *L. complanata*, but *P. grandis* had less biomass at the reach scale given its lower density (Table 2). Tissue and shell C, N, and P content were generally higher for the larger individuals of *P. grandis*, but *L. complanata* showed greater standing stocks of elements at the reach scale due to higher density (Table 2). One exception to this pattern was tissue P abundance at the reach scale, which was higher in *P. grandis* than *L. complanata* (0.043 g m^{-2} and 0.010 g m^{-2}, respectively). For both taxa, P was greater in the tissue than shell (Table 2).

Table 1 Mean (SE) values for water column nutrients, chlorophyll *a* (chl *a*), and seston characteristics

Metric	Mean (SE)
Width (m)	24.7 (3.5)
Depth (cm)	26.3 (0.8)
Discharge (L s^{-1})	923.6
Sp. cond. (μS cm^{-1})	1380
Temperature (°C)	23.4
DO (mg L^{-1})	9.92
DO (%)	119.4
Chl *a* (μg L^{-1})	26.5 (4.0)
Seston (mg L^{-1})	58.7 (16.1)
Seston (% organic)	19.4 (1.8)
Seston C:N (molar)	14.2 (0.1)
Seston N:P (molar)	46.6 (18.8)
Sediment (% organic)	5.15 (1.14)
SRP (μg P L^{-1})	483 (21)
NH_4^+ (μg N L^{-1})	136 (1)
NO_2^- (μg N L^{-1})	70 (3)
NO_3^- (μg N L^{-1})	12,269 (541)
DIN: SRP (molar)	57.1

DO dissolved oxygen, *SRP* soluble reactive phosphorus, NH_4^+ ammonium, NO_2^- nitrite, NO_3^- nitrate

We compared standing stock of C, N, and P at the reach scale in mussel tissue and shells with sediment values (Fig. 1). The total C standing stock in the reach was 41.2 g C m^{-2}, with the largest pool in the sediment (25 g C m^{-2}; 63% of total) and the next largest in *L. complanata* shells (9.8 g C m^{-2}; 28% of total; Fig. 1a). In contrast, sediment accounted for only 24% of total N standing stock and 29% of total P standing stock. The total N standing stock was 1.78 g N m^{-2}, with the majority in *L. complanata* tissue (0.48 g N m^{-2}) and shells (0.48 g N m^{-2}; 54% of total N in tissue + shells). *P. grandis* tissue + shells accounted for 22% of N standing stock (Fig. 1b). In contrast to high N standing stocks in *L. complanata*, *P. grandis* accounted for the largest P pool. The total P standing stock was 0.118 g P m^{-2}, with *P. grandis* tissue at 36% of the total (Fig. 1c).

Feeding and biodeposition rates (Table 3) were generally greater for *P. grandis* than *L. complanata*

Table 2 Mean (SE) number, dry mass (DM), carbon (C), nitrogen (N), and phosphorus (P) for individual mussels (ind^{-1}) of two species, and for mussels scaled to stream density (m^{-2})

	By individual mussel (ind^{-1})		By stream area (m^{-2})	
	L. complanata	*P. grandis*	*L. complanata*	*P. grandis*
Number	10	17	0.96 (0.27)	0.27 (0.03)
Tissue				
DM (g)	2.72 (0.26)	6.10 (0.45)	5.75 (1.84)	2.12 (0.26)
C (g)	1.22 (0.12)	2.45 (0.17)	2.61 (0.84)	0.87 (0.11)
N (g)	0.23 (0.02)	0.43 (0.04)	0.48 (0.15)	0.16 (0.02)
P (g)	0.005 (<0.001)	0.007 (0.001)	0.010 (0.003)	0.043 (0.006)
Shell				
DM (g)	29.18 (3.49)	44.46 (4.34)	70.78 (22.99)	17.84 (2.47)
C (g)	4.24 (0.60)	6.55 (0.67)	9.81 (3.19)	2.64 (0.37)
N (g)	0.21 (0.03)	0.62 (0.11)	0.48 (0.16)	0.24 (0.03)
P (g)	0.001 (<0.001)	0.002 (<0.001)	0.002 (0.001)	0.001 (<0.001)

Table 3 Mean (±SE) values for mussel biodeposition of carbon (C), nitrogen (N), and phosphorous (P), feeding behaviors, as well as ammonium (NH_4^+) excretion for Unionid mussel species in the East Brach of the DuPage River

Mussel feeding and biodeposition	*L. complanata*	*P. grandis*
Total biodeposition rate (mg $stnd^{-1}$ h^{-1})	59.48 (19.64)	128.05 (36.59)
C biodeposition rate (mg $stnd^{-1}$ h^{-1})	5.99 (2.51)	10.41 (3.17)
N biodeposition rate (mg $stnd^{-1}$ h^{-1})	1.82 (0.43)	0.72 (0.22)
P biodeposition rate (mg $stnd^{-1}$ h^{-1})	0.012 (0.005)	0.040 (0.010)
NH_4^+ excretion (mg N gDM^{-1} h^{-1})	10.8 (1.3)	10.0 (1.0)
Feeding		
Clearance rate (L $stnd^{-1}$ h^{-1})	1.83 (0.55)	3.72 (0.77)
Filtration rate (mg $stnd^{-1}$ h^{-1})	56 (16)	114.15 (23.6)
Rejection rate (%)	72.36 (4.43)	71.43 (7.46)
Selection efficiency (fraction)	0.007 (0.006)	0.19 (0.07)
Ingestion rate (mg $stnd^{-1}$ h^{-1})	4.12 (1.45)	8.02 (1.35)
Organic ingested matter (fraction)	0.21 (0.05)	0.23 (0.05)
Absorption rate (mg $stnd^{-1}$ h^{-1})	0.12 (0.11)	3.11 (1.05)
Absorption efficiency (fraction)	0.2 (0.12)	0.32 (0.1)
N-specific feeding		
N filtration rate (mg $stnd^{-1}$ h^{-1})	0.12 (0.04)	0.25 (0.05)
Pseudofeces N production (mg $stnd^{-1}$ h^{-1})	0.23 (0.05)	0.54 (0.14)
N selection efficiency (fraction)	neg	neg
N ingestion rate (mg $stnd^{-1}$ h^{-1})	neg	neg
N absorption rate (mg $stnd^{-1}$ h^{-1})	neg	neg
N absorption efficiency (mg $stnd^{-1}$ h^{-1})	neg	neg
P-specific feeding		
P filtration rate (mg $stnd^{-1}$ h^{-1})	0.009 (0.003)	0.023 (0.005)
Pseudofeces P production (mg $stnd^{-1}$ h^{-1})	6.45×10^{-8} (2.14×10^{-8})	6.05×10^{-8} (8.78×10^{-9})
P selection efficiency (fraction)	neg	neg
P ingestion rate (mg $stnd^{-1}$ h^{-1})	0.013 (0.004)	0.023 (0.005)
P absorption rate (mg $stnd^{-1}$ h^{-1})	0.015 (0.004)	0.022 (0.005)
P absorption efficiency (mg $stnd^{-1}$ h^{-1})	0.95 (0.008)	0.94 (0.012)

For all feeding metrics, N = 10 *L. complanata* and N = 10 *P. grandis* (except NH_4^+ excretion, where N = 3 *L. complanata* and N = 4 *P. grandis*)

neg = when biodeposit N or P > seston

due to its larger size. An exception to this was N biodeposition rate, which showed individuals of *L. complanata* released 1.82 mg $stnd^{-1}$ h^{-1} and *P. grandis* released 0.72 mg $stnd^{-1}$ h^{-1}. Ammonium excretion was similar between species 10–10.8 mg N gDM^{-1} h^{-1} (Table 3). Particle rejection rates were 71–72%, and selection efficiencies were low and variable among individuals. The organic content of the ingested matter was similar to the seston (Table 3), also indicating no selection (i.e. enrichment) of organic matter for ingestion. Many of the N-specific feeding rates were negative (i.e., biodeposit N > seston N), indicating no selection or absorption of N. The P-specific selection efficiency was negative, which corroborates with low particle selection. However, rates of P ingestion and absorption show both species preferentially ingest P (as compared to N), with highly efficient P absorption (94–95%; Table 3).

Mussel effects on sediment composition and fluxes of nutrients and gases

Despite relatively high rates of biodeposition, mussels had no effect on sediment organic matter quantity or

quality in the continuous-flow cores (Table 4). The relative abundance of sediment C, N, P, and the ratios of C:N and N:P were not affected by mussels. However, mussels showed a significant interaction with isotope enrichment for sediment N composition and N:P ratio (2-way ANOVA $p = 0.044$ and $p = 0.006$, respectively; Table 4). The water column ^{15}N addition did not affect sediment characteristics.

The effect of mussels and isotope enrichment were different for the flux of each nutrient (Table 4). Neither factor affected SRP flux, which was consistently directed out of the sediment (Fig. 2a). Flux of NO_2^- was also generally directed out of sediment, and was highest for *P. grandis* relative to *L. complanata* and sediment alone (2-way ANOVA $p = 0.001$; Fig. 2b). Ammonium efflux was also highest with *P. grandis*, intermediate in the *L. complanata*, and showed net uptake in sediment alone (2-way ANOVA $p < 0.001$). Ammonium efflux increased with addition of $^{15}NO_3^-$ relative to $^{15}NH_4^+$ and control (2-way ANOVA $p = 0.037$; Fig. 2c). Finally, NO_3^- flux always showed net uptake, was lower in sediment alone relative to *P. grandis* (2-way ANOVA $p = 0.025$), and was highest with addition of $^{15}NO_3^-$ relative to $^{15}NH_4^+$ and control (2-way ANOVA $p = 0.048$; Table 4; Fig. 2d).

Gas fluxes were affected by both mussels and additions of ^{15}N to the inflow water (Table 4; Fig. 3). Aerobic respiration was higher in both mussel treatments compared to sediment alone (2-way ANOVA $p < 0.001$), and not affected by addition of ^{15}N (2-way ANOVA $p = 0.130$; Fig. 3a). Mean (±SE) O_2 concentration in outflows was 232 (7) μM O_2 with sediment alone, 132 (40) μM O_2 with *L. complanata*, and 93 (54) μM O_2 with *P. grandis*, within the range from studies with live bivalves (Kellogg et al. 2013; Turek and Hoellein 2015). Denitrification was also greater with mussels present than sediment alone (2-way ANOVA $p < 0.001$), and highest with addition of $^{15}NO_3^-$ (2-way ANOVA $p = 0.031$; Table 4;

Table 4 *F*-ratio and p values for 2-way analysis of variance (ANOVA) by mussel treatment (sediment alone, *L. complanata*, and *P. grandis*) and inflow water treatment (no ^{15}N, $+^{15}N$-ammonium, and $+^{15}N$-nitrate; N = 3 for each mussel and inflow water combination) for sediment characteristics, solute fluxes, and gas fluxes

Sediment	Mussel		Water		Interaction	
	F	p value	F	p value	F	p value
Organic matter (%)	1.585	0.234	0.874	0.435	1.163	0.362
C (%)	1.323	0.291	2.345	0.124	0.638	0.642
N (%)	3.292	0.060	0.875	0.434	3.042	**0.044**
P (%)	0.056	0.946	1.647	0.226	0.489	0.744
C:N (molar)	1.973	0.168	0.302	0.743	1.352	0.290
N:P (molar)	1.996	0.168	1.417	0.271	5.317	**0.006**
Chl a (μg cm^{-3})	1.691	0.212	0.140	0.870	1.580	0.223
Solute flux (μg N or P m^{-2} h^{-1})						
SRP	0.446	0.647	0.335	0.720	0.110	0.977
NH_4^+	24.130	**<0.001**	3.975	**0.037**	0.937	0.465
NO_2^-	9.746	**0.001**	2.440	0.115	1.083	0.394
NO_3^-	4.571	**0.025**	3.598	**0.048**	1.029	0.419
DNRA	3.963	0.080	–	–	–	–
Gas flux (μg N or O_2 m^{-2} h^{-1})						
Respiration	70.007	**<0.001**	2.286	0.130	2.123	0.120
Denitrification	14.435	**<0.001**	4.244	**0.031**	2.114	0.121
^{15}N denitrification	43.431	**<0.001**	18.475	**<0.001**	3.325	**0.033**

Bold values are significant at $p \leq 0.050$. *F*-ratio and p values for DNRA and nitrification are from 1-way ANOVA

C carbon, *N* nitrogen, *P* phosphorus, *chl a* chlorophyll *a*, *SRP* soluble reactive phosphorus, NH_4^+ ammonium, NO_2^- nitrite, NO_3^- nitrate, *DNRA* dissimilatory nitrate reduction to ammonium

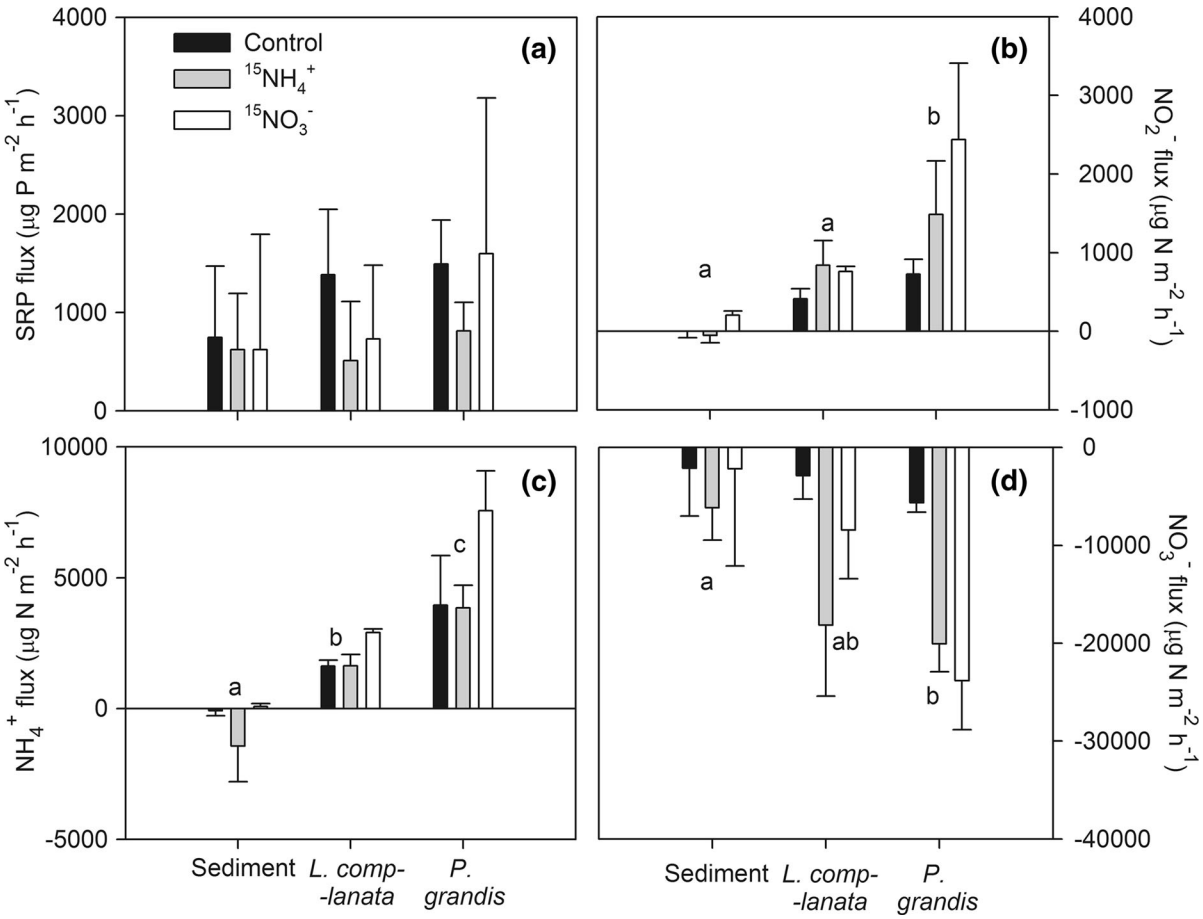

Fig. 2 Mean (±SE) rates of nutrient fluxes with sediment alone, sediment + *L. complanata*, or sediment + *P. grandis* in the continuous-flow cores, and inflow water amended with no isotopes (control), ^{15}N-ammonium ($^{15}NH_4^+$), or ^{15}N-nitrate ($^{15}NO_3^-$; N = 3 per mean). Fluxes are (**a**) soluble reactive phosphorus (SRP), (**b**), nitrite (NO_2^-), (**c**) NH_4^+, or (**d**) NO_3^-. Small letters indicate significant differences among mussel treatments shown by Tukey's post hoc test following a significant effect of mussels in a 2-way ANOVA

Fig. 3b). Finally, there was a significant interaction between type of inflow water and the mussel treatment for production of $^{15}N_2$ (2-way ANOVA $p = 0.003$), so each treatment was analyzed individually (Table 4). With sediment alone, there was no difference in $^{15}N_2$ production with added nutrients, and rates were low. For cores with *L. complanata*, $^{15}N_2$ production was lowest when no ^{15}N was added, higher with addition of $^{15}NH_4^+$, and highest with $^{15}NO_3^-$ addition. Results for *P. grandis* showed the same pattern, except there was only a significant increase of $^{15}N_2$ production with added $^{15}NO_3^-$, and not with added $^{15}NH_4^+$ (Fig. 3c).

Mussels had no effect on DNRA (ANOVA $p = 0.080$; Table 4), although there was a trend of higher rates with *P. grandis* (mean ± SE = 1050 ± 391 µg N m^{-2} h^{-1}) and *L. complanata* (585 ± 191 µg N m^{-2} h^{-1}) relative to sediment alone (46 ± 46 µg N m^{-2} h^{-1}). DNRA was measured in the $+^{15}NO_3^-$ cores, so we compared the relative rates of DNRA and denitrification in that treatment only. The amount of N converted to NH_4^+ via DNRA averaged 2% of denitrification with sediment alone, 12% with *L. complanata* cores, and 8% with *P. grandis*.

Effect of mussels on fluxes at the reach scale

We scaled all DIN fluxes to the stream reach using mussel density measurements to compare the net recycling of N relative to net uptake of N or loss via

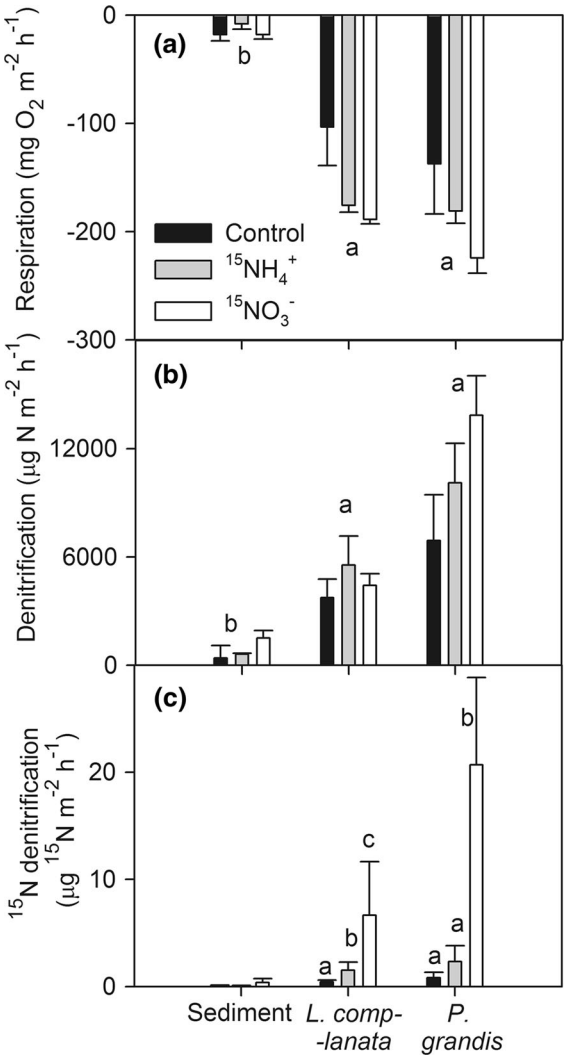

Fig. 3 Mean (±SE) rates of gas fluxes with sediment alone, sediment + *L. complanata*, or sediment + *P. grandis* in the continuous-flow cores, and inflow water amended with no isotopes (control), ^{15}N-ammonium ($^{15}NH_4^+$), or ^{15}N-nitrate ($^{15}NO_3^-$; N = 3 per mean). Fluxes are (**a**) respiration, (**b**) denitrification, and (**c**) denitrification of ^{15}N-labled dinitrogen gas ($^{15}N_2$). Small letters in (**a**) and (**b**) indicate differences in respiration and denitrification among mussel treatments. Small letters in (**c**) indicate differences in ^{15}N denitrification among water treatments for *L. complanata* and *P. grandis* treatments individually, as shown by Tukey's post hoc test following a significant mussel x water interaction effect in a 2-way ANOVA

denitrification, with and without mussels present (Fig. 4). With no mussels, sediments were a net sink of DIN, with the majority in the form of NO_3^- uptake (2.1 mg N m^{-2} h^{-1}), followed by denitrification (0.40 mg N m^{-2} h^{-1}), with low rates of NH_4^+ uptake (0.09 mg N m^{-2} h^{-1}) and NO_2^- uptake (0.001 mg N m^{-2} h^{-1}; Fig. 4). The major changes to DIN fluxes with mussels were net effluxes of NH_4^+, NO_2^-, and biodeposit-N, while production of N_2 increased, and a relatively small mass of N was filtered by mussels (Fig. 4). Because NO_3^- uptake was largely the same across treatments, mussels increased denitrification efficiency (i.e., N_2 production relative to NO_3^- uptake) from 18.6% with no mussels to 130% with *L. complanata* and 122% with *P. grandis*.

Discussion

Mussel standing stock and feeding influence N and P dynamics

Consistent with our hypothesis, mussel tissue and shell represented significant pools of N and P at the reach scale. The relative importance of tissues as long-term sinks varies with the lifespan, life history, density, and persistence of spent shells (Atkinson et al. 2016; Vanni et al. 2013). Both *P. grandis* and *L. complanata* have

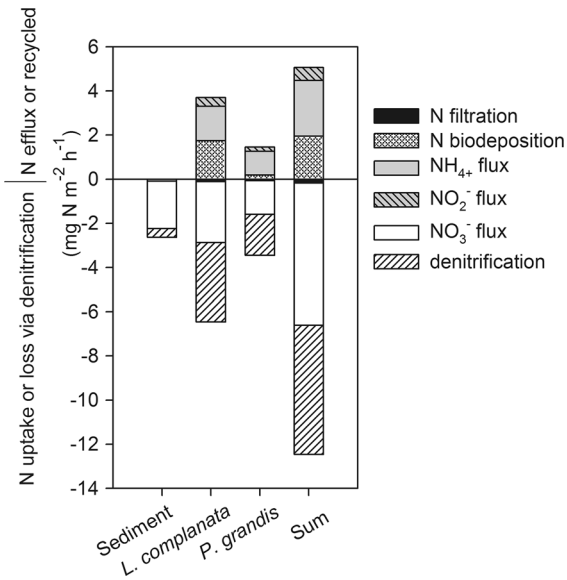

Fig. 4 Microbial- and mussel-mediated fluxes of nitrogen (N) at the stream reach scale for sediment alone, *L. complanata* + sediment, *P. grandis* + sediment, and both mussel taxa + sediment (sum). Uptake of N, mussel N filtration, and loss via denitrification are shown as negative values, and recycling of N into other biologically active forms are shown as positive values (e.g., biodeposition). NH_4^+ ammonium, NO_2^- nitrite, NO_3^- nitrate

opportunistic life history, with rapid growth, early sexual maturity, and lifespans of 11–19 years (Anthony et al. 2001; Haag 2012). Shells of dead individuals decay according to a variety of intrinsic (i.e., chemical structure) and extrinsic factors (e.g., pH). Among the latter, water velocity and calcium carbonate are critical (Strayer and Malcom 2007). Our study site has relatively slow moving flow and water in this region is typically alkaline so shells may be long-lasting. Thus, Unionid tissues and shell are potentially significant and overlooked nutrient sinks in this urban river.

Feeding and biodeposition results showed distinct patterns for N and P, which may reflect the generally high DIN:SRP ratio of water column concentrations, and are consistent with previous stoichiometric analyses on Unionidae (Christian et al. 2008). Both mussel species had tissue C:N ratios consistent with the Redfield ratio (i.e., 6.6). However, N was greater in the feces and pseudofeces than in the seston, resulting in negative N-specific feeding rates and suggesting N-replete conditions in the tissue. In contrast, both taxa had very low P content and the tissue and seston N:P ratios were well above the Redfield ratio. The mussels seemed to respond to this condition by modifying post-ingestion processes, particularly through high P absorption relative to P ingestion (i.e., absorption efficiency $\sim$95%). An alternative feeding mechanism that could have enhanced P acquisition is the selection of P-rich particles for ingestion, but mussels did not show any particle selection. Christian et al. (2008) suggested N or P limitation in mussels would be evident from low N and P in biodeposits. In our study, the water chemistry, seston, mussel N and P content, and nutrient-specific feeding and biodeposition rates all suggest mussels were N-replete and P-limited, and thus biodeposits were high in N and low in P. These data suggest that mussel feeding could enhance overall P retention, an important component of nutrient management in this urban watershed. Human activities are increasing available N relative to P in freshwaters globally (Beusen et al. 2016). Studies like the present work contribute to our collective understanding of how the stoichiometry of eutrophic waters may affect species targeted for restoration in nutrient-enriched ecosystems.

Our study represents the first application of the biodeposition method for measuring feeding rates in freshwater mussels, but we have confidence in the results given similarities to other well-studied marine bivalves using the same method (Bayne 2002; Galimany et al. 2013; Hoellein et al. 2015). Overall, there are few measurements of feeding behaviors of freshwater mussels, so these data make a significant contribution to the field. Previous estimates of Unionid clearance rates are variable, with some lower than our results at <0.1 l h^{-1} gDW^{-1} (Cahoon and Owen 1996; Spooner and Vaughn 2008) and others similar (Baker and Levinton 2003; Kryger and Riisgård 1988). Variation in clearance rates among studies may be attributed to measurement method, food quality and quantity, and life history. In addition, some Unionid species may use a mixture of suspension and deposit feeding, so seston-based clearance rates may not offer a complete view of in situ feeding activity for some taxa. For example, Raikow and Hamilton (2001) showed deposit material can account for 80% of Unionids' diet in a Michigan stream. Given the importance of Unionid feeding to the ecosystem services of biofiltration and nutrient cycling (Vaughn et al. 2015), additional studies that integrate approaches, such as the biodeposition method and stable isotopes, are needed to further understand Unionid contributions to nutrient retention and ecosystem services, and thereby inform mussel conservation efforts.

Net fluxes of NH_4^+ and NO_3^- by mussels suggest they have a major role in providing DIN for benthic N demand, despite high water column DIN concentrations. The net NH_4^+ flux with mussels present (*L. complanta* = 1621 µg N m^{-2} h^{-1}, *P. grandis* = 3950 µg N m^{-2} h^{-1}) was much greater than net NH_4^+ uptake in sediments without mussels (90 µg N m^{-2} - h^{-1}), and in the same range as rates of net NO_3^- uptake (2156–5650 µg N m^{-2} h^{-1}). The NH_4^+ in mussel cores can originate from NH_4^+ excretion, biodeposits, sediment mineralization, desorption, and DNRA. Other studies measuring DIN flux from live bivalves in cores have shown significant effluxes of NH_4^+ including measurements with oysters (Smyth et al. 2013) and clams (Turek and Hoellein 2015), at rates higher than net benthic uptake of NH_4^+ and NO_3^-. In addition, Atkinson et al. (2014) fed ^{15}N-labeled food to Unionid mussels and found that mussel-derived N supplied 40% of total N demand and up to 74% of N in the stream food web. Similar patterns have been documented for other consumers (e.g., amphibians and macroinvertebrates)

which made significant contributions to overall stream DIN demand (Benstead et al. 2010; Griffiths and Hill 2014; Keitzer and Goforth 2013).

It is often assumed that consumers have the strongest influence on nutrient dynamics under conditions where ecosystem processes are nutrient limited (Capps and Flecker 2013; Small et al. 2011; Vanni 2002), therefore high nutrient concentrations in eutrophic habitats would override the importance of consumers (but see Vanni et al. 2006). However, this may not be true in eutrophic streams, which have relatively low water volume to surface area compared to other habitats such as large rivers, lakes, and coastal ecosystems. In addition, while eutrophication reduces species richness in streams, those taxa tolerant of eutrophic conditions can be present in very high densities (Walsh et al. 2005), such as Chironomidae (midges), aquatic crustaceans (Gammaridae and Asellidae), and bivalves including C. *fluminea*. For example, density of *C. fluminea* in the eutrophic North Branch of the Chicago River was 1514 individuals m^{-2}, and clams at that site increased denitrification to a greater degree than clams in a low nutrient stream (Turek and Hoellein 2015). Similarly, both Unionid species in this study are considered generalists which are tolerant of eutrophic conditions and widespread in the upper Midwestern US (Haag 2012). Given their high density and tolerance to poor water quality, the role of consumers on nutrient dynamics in eutrophic streams may be overlooked, and greater scrutiny of their capacity to remove excess nutrients from aquatic environments is warranted.

Mussel effect on N_2 fluxes and pathways

Our results clearly showed mussels significantly increased denitrification rates, with the most likely explanation being an increase in NO_3^- movement from the water column to sediment. Primary controls on denitrification include redox conditions, organic matter, and NO_3^- (Groffman et al. 1999). We can rule out differences in sediment redox state as an explanation using the patterns in sediment respiration (Fig. 2). Mussels increased respiration (i.e., consumed oxygen) relative to sediment alone, but the patterns were identical for both species and for all water column treatments. In contrast, denitrification was significantly higher with *P. grandis* compared to *L. complanata*, and was higher across all treatments with added $^{15}NO_3^-$. In addition, we can exclude differences in organic matter quantity and quality as an explanation for increased denitrification as there were no differences among cores with sediments and mussels, or among water column treatments (Table 4). Thus, changes in NO_3^- concentration or movement are the most likely explanation for denitrification results. The NO_3^- used for denitrification can originate via nitrification or the water column. While we did not measure nitrification directly, we note that denitrification represented 19% of NO_3^- uptake in sediment alone and 122–130% of NO_3^- uptake with Unionids added. Thus, some portion of N_2 production was likely subsidized from nitrification. While some denitrification can occur in bivalve guts and shell biofilms (Svenningsen et al. 2012), we assumed this to be minor relative to sediment fluxes. Overall, we conclude that mussel movement, including filtration and burrowing, enhanced the delivery of water column NO_3^- to sediment microbes, which was the primary mechanism for increased denitrification rates. The relative effect of Unionids on coupled nitrification–denitrification is unknown, possibly important, and should be included in future studies.

Other infaunal bivalves increase denitrification more than sediment alone, but patterns vary depending on environmental conditions. Using identical continuous-flow cores as this study, Turek and Hoellein (2015) found higher net N_2 flux and denitrification efficiency in sediment cores with live *C. fluminea* relative to sediment alone or sediment that had been exposed to *C. fluminea* in an urban river. The effect of *C. fluminea* was greater in a high nutrient stream relative to a low-nutrient stream, as more NO_3^- was available in the former. In a similar fashion, the burrowing cockle *Austrovenus stutchbury* increased denitrification potential in a shallow marine environment, most likely through bioturbation which promoted coupled nitrification–denitrification of N from excreted NH_4^+ (Jones et al. 2011). However, the relative effect of *A. stutchbury* was limited in organic-rich sediments which were less likely to show C- and N-limitation of denitrification potential. Finally, the Unoinid *Sinanodonta woodiana*, invasive in Europe, increased flux of NH_4^+, N_2, and methane in sediments from a stream in Italy, which the authors suggested had important implications for biogeochemistry at the reach scale (Benelli et al. 2017).

The role of hydrology on dispersal of biodeposits from bivalves may also drive their capacity to deliver C and N to sediment denitrifiers. In lentic habitats, biodeposits may sink directly within the bivalve colonies, where nutrients can be concentrated in sediments. For example, Bruesewitz et al. (2006, 2009) showed zebra mussels (*D. polymorpha*; an epifaunal mussel) reduced NO_3^- limitation of denitrification, likely via nitrification of biodeposits in lentic habitats. However, biodeposits from bivalves in flowing-water ecosystems may be dispersed by currents to downstream habitats (Atkinson et al. 2014). This relative importance of bioturbation and biodeposits for increased denitrification rates with bivalves has not yet been tested empirically, but is a promising approach for research syntheses across taxa and ecosystems.

Relative role of DNRA in N cycling

Simultaneous comparisons of DNRA to other N transformation rates are useful to determine whether stream sediments recycle N (via DNRA) or remove N (via denitrification), from the context of dissimilatory NO_3^- cycling. Research on relative importance of DNRA in the N cycling of streams has focused on hyporheic sediments, fermentive processes, and activity of sulfur (S) oxidizing, chemolithoautotrophic bacteria (Burgin and Hamilton 2008; Storey et al. 2004). Comparing DNRA to net NO_3^- uptake from the $+^{15}NO_3^-$ cores in this study suggest relatively little NO_3^- is used for DNRA, with mean (±SE) estimates of 0.2 (0.2)% (sediment alone), 4.9 (2.9)% (*L. complanata*), and 5.3 (2.3) % (*P. grandis*). We also compared the rates of DNRA to denitrification (as percentage) in the $^{15}NO_3^-$ cores, where DNRA represented a mean of 2.4–12.4% of denitrification. Overall, we conclude that DNRA was relatively minor component of net NO_3^- uptake, DNRA tended to be higher with mussel presence (but not significantly so), and rates of DNRA are much lower than denitrification. We note these measurements were conducted with cores composed of previously homogenized riverine sediment with added $^{15}NO_3^-$, which may obscure natural gradients of N, S, and C compounds and favor denitrification over DNRA (Morkved et al. 2005). Also, we did not measure S solutes, but some S species were likely present given the proximity to upstream impoundments and wetlands. Understanding the role of DNRA in streams would benefit from assessment of microbial communities and gene abundances for each metabolic pathway (Burgin and Hamilton 2008; Lindemann et al. 2016).

Ecosystem services: value of mussel-enhanced denitrification

We followed the calculations from Beseres-Pollack et al. (2013), which are based on oysters' role in N retention, to estimate the economic value of N loss via Unionid-enhanced denitrification. First, we estimated the mass of N loss per area (kg N m^{-2}) for the entire East Branch of the DuPage River assuming length of 41.9 km and mean width of 15 m (benthic area = 628,500 m^2). We used mean denitrification values for sediment, *L. complanata* and *P. grandis*, along with density (No. m^{-2}) to calculate N loss. For example, multiplying the denitrification rate with *L. complanata* alone by density and river area gives the daily mass of *L. complanata* mediated-denitrification at the river scale:

$$0.0897 \text{ g N m}^{-2}\text{d}^{-1} \times 0.97 \text{ m}^{-2} \times 628{,}500 \text{ m}^2 = 56 \text{ kg N d}^{-1}$$

Beseres-Pollack et al. (2013) showed the Black River wastewater treatment plant (WWTP) in Maryland removes 15,260 kg N d^{-1} while treating 180 million gal d^{-1} of wastewater. We calculated the equivalent volume for a WWTP with the capacity to remove the same amount of N as *L. complanata*-enhanced denitrification using the proportion:

$$15{,}260 \text{ kg N d}^{-1}/180 \text{ million gal d}^{-1} = 56 \text{ kg N d}^{-1}/\text{x million gal d}^{-1}$$

where solving for x indicates 0.67 million gal d^{-1}. Beseres-Pollack et al. (2013) reported the capital cost of the WWTP is $2,975,631 for each million gal d^{-1} capacity. We calculated the cost of a WWTP to treat the same amount of N lost via L. *complanata*-mediated denitrification as:

$$0.67 \text{ million gal d}^{-1} \times \$2{,}975{,}361 \text{ per million gal d}^{-1} = \$1{,}979{,}652$$

Beseres-Pollack et al. (2013) converted this value to an annual cost by estimating the WWTP life span at 15 years (straight-line depreciation with no scrap

value) with 2% maintenance and operation costs per year. Calculated for *L. complanata*-mediated N loss:

$$(\$1,979,652/15\,y) + (\$1,979,652 \times 0.02) = \$171,562\,y^{-1}$$

We repeated all calculations for the value of *P. grandis*-mediated denitrification ($95,077) and denitrification by sediment alone ($18,078). Together, the two Unionid taxa could yield a maximum potential of contributing to $266,638 of N loss per year via denitrification in the East Branch DuPage River.

This estimation has four critical assumptions that require further explanation to interpret results: (1) the value for mussel-mediated denitrification is the same over the course of the year (our measurements reflect only a single date in June), (2) mussel density is the same at the scale of the entire river as we measured at the study site, (3) effects of mixed-species assemblages on denitrification rates is the same as single species assemblages, and (4) the N reduction which occurs in a WWTP (i.e., very high N concentrations in raw sewage decreased to moderate N concentrations in effluent to the river) would have the same infrastructure cost as the N reduction that occurs in situ (i.e., reducing the moderate N concentrations the mussels are exposed to in the river). For the first assumption, we note that denitrification can be seasonally variable including changes in temperature and NO_3^- availability, although models of seasonal trends are lacking. For the second, we calculated the dollar-value of N loss across a range of more realistic *L. complanata* and *P. grandis* densities (i.e., lower values) at the scale of the entire river benthos, where the maximum was our reach densities of 0.96 and 0.27 individual m^{-2}, respectively, and the minimum was 1% of each value at the scale of the entire river (Fig. 5). Unionids in mixed species assemblages could offer complementary effects on nutrient cycling via species-specific patterns in feeding, excretion, and burrowing. However, the effects of mixed species on N cycling have not been measured. Finally, WWTPs are designed to reduce very high nutrient loads to moderate loads, while mussel-enhanced denitrification in the river is a more difficult task: to reduce comparatively low (but still eutrophic) N concentrations to even lower concentrations. It's possible that designing WWTP that can enhance denitrification at lower N and C levels may be more expensive than the values reported here, thereby undervaluing mussels role in N removal relative to infrastructure cost.

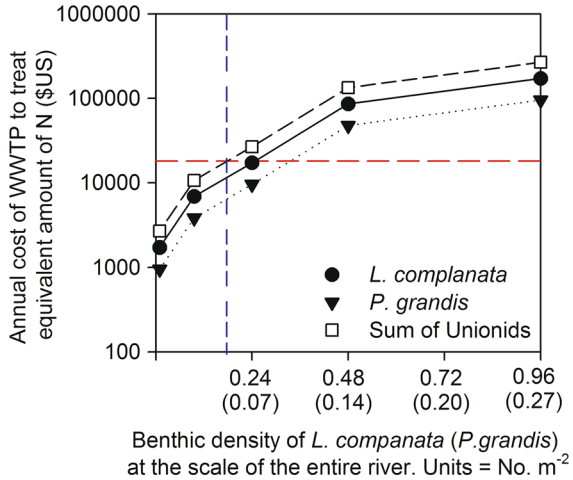

Fig. 5 The annual cost for the construction and maintenance of a wastewater treatment plant (WWTP) to treat the same amount of nitrogen (N) as denitrified by Unionid mussels *L. complanata* and *P. grandis* in the East Branch DuPage River. Dollar values vary according to projections of mussel density at the scale of the entire river, shown here where the maximum is the density at the study reach (0.96 m^{-2} for *L. complanata* and 0.27 m^{-2} for *P. grandis*). The horizontal dashed indicates the annual value of N loss via sediment denitrification at the scale of the entire river ($18,078). The vertical dashed line indicates the *L. complanata* and *P. grandis* densities required at the scale of the entire river to double denitrification by sediment alone

There are no data on mussel density or assemblage at the river scale for the DuPage River, so we present financial projections in Fig. 5 to inform the goals for restoration or conservation of mussel taxa, and to help place expenses in context of possible benefits across a range of mussel densities. For example, one goal of mussel restoration may be to increase denitrification from sediment alone in the river by a factor of two (i.e., to double the amount of denitrification in the river). This could be achieved if the entire river had ~16% of the mussel density measured at our study reach (0.16 individual m^{-2} *L. complanata* and 0.04 individual m^{-2} *P. grandis* at the river scale), which would provide a value of approximately $18,000 $year^{-1}$ in N loss via denitrification (Fig. 5). This target mussel density may be feasible, as Holland-Bertels (1990) found 0.12 individual m^{-2} for *L. complanata* and 0.4 individual m^{-2} for *P. grandis* in the Upper Mississippi River (East Channel, Pool 10). Managers may be

better positioned to find the political and economic support for protection or restoration of mussel populations with economic projections of mussels' ecosystem benefits. However, we acknowledge our estimates for the economic value of Unionid-mediated denitrification are preliminary, and refinement will require seasonal measurements of N fluxes, river-scale assessments of bivalve density, and tests of single and mixed species assemblages on sediment biogeochemistry. Future studies can expand upon this empirical foundation to contribute calculations for the ecosystem services provided by freshwater mussel communities.

Acknowledgements Funding was provided by Loyola University Chicago and the National Science Foundation (MRI-0959876). For assistance in the laboratory we thank Melaney Dunne, Michael Hassett, Ashley Cook, Amanda McCormick, and Samantha Hertel from Loyola University Chicago and Erika Fusco, Monzural Haque, and Siena Schickler from Baruch College. We thank Rebecca Chmiel, Emma Berger, and Whitney King at Colby College.

References

An S, Gardner WS, Kana T (2001) Simultaneous measurement of denitrification and nitrogen fixation using isotope pairing with membrane inlet mass spectormetry analysis. Appl Environ Microbiol 67(3):1171–1178

Anthony JL, Kesler DH, Downing WL, Downing JA (2001) Length-specific growth rates in freshwater mussels (Bivalvia: Unionidae): extreme longevity or generalized growth cessation? Freshw Biol 46(10):1349–1359

APHA (1998) Standard methods for the examination of water and wastewater, 20th edn. United Book Press Inc, Baltimore, MD

Aspila K, Agemian H, Chau A (1976) A semi-automated method for the determination of inorganic, organic and total phosphate in sediments. Analyst 101(1200):187–197

Atkinson CL, Vaughn CC (2015) Biogeochemical hotspots: temporal and spatial scaling of the impact of freshwater mussels on ecosystem function. Freshw Biol 60(3):563–574

Atkinson CL, Kelly JF, Vaughn CC (2014) Tracing consumer-derived nitrogen in riverine food webs. Ecosystems 17(3):485–496

Atkinson CL, Capps KA, Rugenski AT, Vanni MJ (2016) Consumer-driven nutrient dynamics in freshwater ecosystems: from individuals to ecosystems. Biol Rev. doi:10.1111/brv.12318

Baker SM, Levinton JS (2003) Selective feeding by three native North American freshwater mussels implies food competition with zebra mussels. Hydrobiologia 505(1–3):97–105

Bayne BL (2002) A physiological comparison between Pacific oysters *Crassostrea gigas* and Sydney Rock oysters *Saccostrea glomerata*: food, feeding and growth in a shared habitat. Mar Ecol Prog Ser 232:163–178

Bayne BL, Hedgecock D, McGoldrick D, Rees R (1999) Feeding behaviour and metabolic efficiency contribute to growth heterosis in Pacific oysters *Crassostrea gigas* (Thunberg). J Exp Mar Biol Ecol 233(1):115–130

Beaulieu JJ, Tank JL, Hamilton SK, Wollheim WM, Hall RO, Mulholland PJ, Peterson BJ, Ashkenas LR, Cooper LW, Dahm CN, Dodds WK, Grimm NB, Johnson SL, McDowell WH, Poole GC, Valett HM, Arango CP, Bernot MJ, Burgin AJ, Crenshaw CL, Helton AM, Johnson LT, O'Brien JM, Potter JD, Sheibley RW, Sobota DJ, Thomas SM (2011) Nitrous oxide emission from denitrification in stream and river networks. Proc Natl Acad Sci USA 108(1):214–219

Beck MW, Brumbaugh RD, Airoldi L, Carranza A, Coen LD, Crawford C, Defeo O, Edgar GJ, Hancock B, Kay MC, Lenihan HS, Luckenbach MW, Toropova CL, Zhang G, Guo X (2011) Oyster reefs at risk and recommendations for conservation, restoration, and management. Bioscience 61(2):107–116

Benelli S, Bartoli M, Racchetti E, Moraes PC, Zilius M, Lubiene I, Fano EA (2017) Rare but large bivalves alter benthic respiration and nutrient recycling in riverine sediments. Aquat Ecol 51(1):1–16

Benstead JP, Cross WF, March JG, McDowell WH, Ramirez A, Covich AP (2010) Biotic and abiotic controls on the ecosystem significance of consumer excretion in two contrasting tropical streams. Freshw Biol 55(10):2047–2061

Beseres Pollack J, Yoskowitz D, Kim HC, Montagna PA (2013) Role and value of nitrogen regulation provided by oysters (*Crassostrea virginica*) in the Mission-Aransas Estuary, Texas, USA. PLoS ONE 8(6):e65314

Beusen AH, Bouwman AF, Van Beek LP, Mogollón JM, Middelburg JJ (2016) Global riverine N and P transport to ocean increased during the 20th century despite increased retention along the aquatic continuum. Biogeosciences 13(8):2441

Bruesewitz DA, Tank JL, Bernot MJ, Richardson WB, Strauss EA (2006) Seasonal effects of the zebra mussel (*Dreissena polymorpha*) on sediment denitrification rates in Pool 8 of the Upper Mississippi River. Can J Fish Aquat Sci 63(5):957–969

Bruesewitz DA, Tank JL, Bernot MJ (2008) Delineating the effects of zebra mussels (*Dreissena polymorpha*) on N transformation rates using laboratory mesocosms. J N Am Benthol Soc 27(2):236–251

Bruesewitz DA, Tank JL, Hamilton SK (2009) Seasonal effects of zebra mussels on littoral nitrogen transformation rates in Gull Lake, Michigan, USA. Freshw Biol 54(7):1427–1443

Bruesewitz DA, Gardner WS, Mooney RF, Pollard L, Buskey EJ (2013) Estuarine ecosystem function response to flood and drought in a shallow, semiarid estuary: nitrogen cycling and ecosystem metabolism. Limnol Oceanogr 58(6):2293–2309

Bruesewitz DA, Gardner WS, Mooney RF, Buskey EJ (2015) Seasonal water column NH_4^+ cycling along a semi-arid subtropical river–estuary continuum: responses to episodic events and drought conditions. Ecosystems 18(5):792–812

Burgin AJ, Hamilton SK (2008) NO_3^--driven SO_4^{2-} production in freshwater ecosystems: implications for N and S cycling. Ecosystems 11(6):908–922

Cahoon L, Owen D (1996) Can suspension feeding by bivalves regulate phytoplankton biomass in Lake Waccamaw, North Carolina? Hydrobiologia 325(3):193–200

Capps KA, Flecker AS (2013) Invasive fishes generate biogeochemical hotspots in a nutrient-limited system. PLoS ONE 8(1):e54093

Christian AD, Crump BG, Berg DJ (2008) Nutrient release and ecological stoichiometry of freshwater mussels (Mollusca: Unionidae) in 2 small, regionally distinct streams. J N Am Benthol Soc 27(2):440–450

DuPage County Stormwater Management (2015) East Branch DuPage River Watershed and Resiliency Plan. The County of DuPage, Wheaton, IL

Eyre BD, Rysgaard S, Dalsgaard T, Christensen PB (2002) Comparison of isotope pairing and N2: Ar methods for measuring sediment denitrification—Assumption, modifications, and implications. Estuaries 25(6):1077–1087

Galimany E, Rose JM, Dixon MS, Wikfors GH (2013) Quantifying feeding behaviors of ribbed mussels, *Geukensia demissa*, in two urban sites (Long Island Sound, USA) with different seston conditions. Estuar Coasts 36:1265–1273

Gardner WS, McCarthy MJ (2009) Nitrogen dynamics at the sediment-water interface in shallow, sub-tropical Florida Bay: why denitrification efficiency may decrease with increased eutrophication. Biogeochemistry 95(2–3):185–198

Gardner WS, McCarthy MJ, Carini SA, Souza AC, Lijun H, McNeal KS, Puckett MK, Pennington J (2009) Collection of intact sediment cores with overlying water to study nitrogen-and oxygen-dynamics in regions with seasonal hypoxia. Cont Shelf Res 29(18):2207–2213

Grabowski JH, Peterson CH (2007) Restoring oyster reefs to recover ecosystem services. In: Cuddington K, Byers JE, Wilson WG, Hastings A (eds) Ecosystem engineers: plants to protists. Academic Press, Amsterdam, pp 281–298

Griffiths NA, Hill WR (2014) Temporal variation in the importance of a dominant consumer to stream nutrient cycling. Ecosystems 17(7):1169–1185

Groffman PM, Holland EA, Myrold DD, Robertson GP, Zou X (1999) Denitrification. In: Robertson GP (ed) Standard soil methods for long-term ecological research. Oxford University Press, Cary, NC, pp 272–290

Haag WR (2012) North American freshwater mussels: natural history, ecology, and conservation. Cambridge University Press, New York, NY

Hall R, Tank JL, Dybdahl MF (2003) Exotic snails dominate nitrogen and carbon cycling in a highly productive stream. Front Ecol Environ 1(8):407–411

Heisterkamp IM, Schramm A, Larsen LH, Svenningsen NB, Lavik G, de Beer D, Stief P (2013) Shell biofilm-associated nitrous oxide production in marine molluscs: processes, precursors and relative importance. Environ Microbiol 15(7):1943–1955

Hoellein TJ, Zarnoch CB (2014) Effect of eastern oysters (*Crassostrea virginica*) on sediment carbon and nitrogen dynamics in an urban estuary. Ecol Appl 24(2):271–286

Hoellein TJ, Zarnoch CB, Grizzle R (2015) Eastern oyster (*Crassostrea virginica*) filtration, biodeposition, and sediment nitrogen cycling at two oyster reefs with contrasting water quality in Great Bay Estuary (New Hampshire, USA). Biogeochemistry 122(1):113–129

Holland-Bartels LE (1990) Physical factors and their influence on the mussel fauna of a main channel border habitat of the upper Mississippi River. J N Am Benthol Soc 9(4):327–335

Iglesias JIP, Urrutia MB, Navarro E, Ibarrola I (1998) Measuring feeding and absorption in suspension-feeding bivalves: an appraisal of the biodeposition method. J Exp Mar Biol Ecol 219(1–2):71–86

Inwood SE, Tank JL, Bernot MJ (2005) Patterns of denitrification associated with land use in 9 midwestern headwater streams. J N Am Benthol Soc 24(2):227–245

Janetski DJ, Chaloner DT, Tiegs SD, Lamberti GA (2009) Pacific salmon effects on stream ecosystems: a quantitative synthesis. Oecologia 159(3):583–595

Jones HFE, Pilditch CA, Bruesewitz DA, Lohrer AM (2011) Sedimentary environment influences the effect of an infaunal suspension feeding bivalve on estuarine ecosystem function. PLoS ONE 6(10):e27065

Kana TM, Weiss DL (2004) Comment on "Comparison of isotope pairing and N_2:Ar methods for measuring sediment denitrification" by B. D. Eyre, S. Rysgaard, T. Dalsgaard, and P. Bondo Christensen. 2002. Estuaries 25:1077–1087. Estuaries 27(1):173–176

Kana TM, Sullivan MB, Cornwell JC, Groszkowski KM (1998) Denitrification in estuarine sediments determined by membrane inlet mass spectrometry. Limnol Oceanogr 43(2):334–339

Keitzer SC, Goforth RR (2013) Spatial and seasonal variation in the ecological significance of nutrient recycling by larval salamanders in Appalachian headwater streams. Freshw Sci 32(4):1136–1147

Kellogg LM, Cornwell JC, Owens MS, Paynter KT (2013) Denitrification and nutrient assimilation on a restored oyster reef. Mar Ecol Prog Ser 480:1–19

Kellogg ML, Smyth AR, Luckenbach MW, Carmichael RH, Brown BL, Cornwell JC, Piehler MF, Owens MS, Dalrymple DJ, Higgins CB (2014) Use of oysters to mitigate eutrophication in coastal waters. Estuar Coast Shelf Sci 151:156–168

Kryger J, Riisgård HU (1988) Filtration rate capacities in 6 species of European freshwater bivalves. Oecologia 77(1):34–38

Levi PS, Tank JL, Tiegs SD, Chaloner DT, Lamberti GA (2013) Biogeochemical transformations of a nutrient subsidy: salmon, streams, and nitrification. Biogeochemistry 113:643–655

Lindemann S, Zarnoch CB, Castignetti D, Hoellein TJ (2016) Effect of eastern oysters (*Crassostrea virginica*) and seasonality on nitrite reductase gene abundance (*nirS*, *nirK*, *nrfA*) in an urban estuary. Estuar Coasts 39(1):218–232

Lydeard C, Cowie RH, Ponder WF, Bogan AE, Bouchet P, Clark SA, Cummings KS, Frest TJ, Gargominy O, Herbert DG (2004) The global decline of nonmarine mollusks. Bioscience 54(4):321–330

McCarthy MJ, Gardner WS (2003) An application of membrane inlet mass spectrometry to measure denitrification in a recirculating mariculture system. Aquaculture 218(1–4):341–355

McCarthy MJ, Gardner WS, Lavrentyev PJ, Moats KM, Joehem FJ, Klarer DM (2007) Effects of hydrological flow regime on sediment-water interface and water column nitrogen

dynamics in a great lakes coastal wetland (Old Woman Creek, Lake Erie). J Great Lakes Res 33(1):219–231

McCarthy MJ, McNeal KS, Morse JW, Gardner WS (2008) Bottom-water hypoxia effects on sediment–water interface nitrogen transformations in a seasonally hypoxic, shallow bay (Corpus Christi Bay, TX, USA). Estuar Coasts 31(3):521–531

McIntyre PB, Flecker AS, Vanni MJ, Hood JM, Taylor BW, Thomas SA (2008) Fish distributions and nutrient cycling in streams: can fish create biogeochemical hotspots. Ecology 89(8):2335–2346

Morkved P, Sovik A, Klove B, Bakken L (2005) Removal of nitrogen in different wetland filter materials: use of stable nitrogen isotopes to determine factors controlling denitrification and DNRA. Water Sci Technol 51(9):63–71

Murphy J, Riley JP (1962) A modified single solution method for determination of phosphate in natural waters. Anal Chim Acta 26(1):31–36

Parsons TR, Maita Y, Lalli CM (1984) A manual of chemical and biological methods for seawater analysis. Pergamon Press, New York, NY

Raikow DF, Hamilton SK (2001) Bivalve diets in a midwestern US stream: a stable isotope enrichment study. Limnol Oceanogr 46(3):514–522

Small GE, Pringle CM, Pyron M, Duff JH (2011) Role of the fish *Astyanax aeneus* (Characidae) as a keystone nutrient recycler in low-nutrient Neotropical streams. Ecology 92(2):386–397

Smyth AR, Geraldi NR, Piehler MF (2013) Oyster-mediated benthic-pelagic coupling modifies nitrogen pools and processes. Mar Ecol Prog Ser 493:23–30

Smyth AR, Piehler MF, Grabowski JH (2015) Habitat context influences nitrogen removal by restored oyster reefs. J Appl Ecol 52(3):716–725

Solorzano L (1969) Determination of ammonium in natural waters by the phenolhypochlorite method. Limnol Oceanogr 14:799–801

Spooner DE, Vaughn CC (2008) A trait-based approach to species' roles in stream ecosystems: climate change, community structure, and material cycling. Oecologia 158(2):307–317

Storey RG, Williams DD, Fulthorpe RR (2004) Nitrogen processing in the hyporheic zone of a pastoral stream. Biogeochemistry 69(3):285–313

Strayer DL (2014) Understanding how nutrient cycles and freshwater mussels (Unionoida) affect one another. Hydrobiologia 735(1):277–292

Strayer DL, Malcom HM (2007) Shell decay rates of native and alien freshwater bivalves and implications for habitat engineering. Freshw Biol 52(8):1611–1617

Strayer DL, Caraco NF, Cole JJ, Findlay S, Pace ML (1999) Transformation of freshwater ecosystems by bivalves. Bioscience 49(1):19–27

Svenningsen NB, Heisterkamp IM, Sigby-Clausen M, Larsen LH, Nielsen LP, Stief P, Schramm A (2012) Shell biofilm nitrification and gut denitrification contribute to emission of nitrous oxide by the invasive freshwater mussel *Dreissena polymorpha* (zebra mussel). Appl Environ Microbiol 78(12):4505–4509

Turek KA, Hoellein TJ (2015) The invasive Asian clam (*Corbicula fluminea*) increases sediment denitrification and ammonium flux in 2 streams in the Midwestern United States. Freshw Sci 34(2):472–484

Vanni MJ (2002) Nutrient cycling by animals in freshwater ecosystems. Annu Rev Ecol Syst 33:341–370

Vanni MJ, Bowling AM, Dickman EM, Hale RS, Higgins KA, Horgan MJ, Knoll LB, Renwick WH, Stein RA (2006) Nutrient cycling by fish supports relatively more primary production as lake productivity increases. Ecology 87(7):1696–1709

Vanni MJ, Boros G, McIntyre PB (2013) When are fish sources vs. sinks of nutrients in lake ecosystems? Ecology 94(10):2195–2206

Vaughn CC, Hakenkamp CC (2001) The functional role of burrowing bivalves in freshwater ecosystems. Freshw Biol 46(11):1431–1446

Vaughn CC, Nichols SJ, Spooner DE (2008) Community and foodweb ecology of freshwater mussels. J N Am Benthol Soc 27(2):409–423

Vaughn CC, Atkinson CL, Julian JP (2015) Drought-induced changes in flow regimes lead to long-term losses in mussel-provided ecosystem services. Ecol Evol 5(6):1291–1305

Walsh CJ, Roy AH, Feminella JW, Cottingham PD, Groffman PM, Morgan RP (2005) The urban stream syndrome: current knowledge and the search for a cure. J N Am Benthol Soc 24(3):706–723

Welsh DT, Nizzoli D, Fano EA, Viaroli P (2014) Direct contribution of clams (*Ruditapes philippinarum*) to benthic fluxes, nitrification, denitrification and nitrous oxide emission in a farmed sediment. Estuar Coast Shelf Sci 154:84–93

Zar JH (1999) Biostatistical analysis. Prentice-Hall Inc, Upper Saddle River, NJ

Zhang L, Shen Q, Hu H, Shao S, Fan C (2011) Impacts of *Corbicula fluminea* on oxygen uptake and nutrient fluxes across the sediment-water interface. Water Air Soil Pollut 220(1–4):399–411